

Electronic Supplementary Information

**Engineering Surface Ligands of Nanocrystals to Design High
Performance Strain Sensor Arrays through All solution Processes**

S.-W. Lee, H. Joh, M. Seong, W. S. Lee, J.-H. Choi and S. J. Oh*

Derivation of the equation to calculate gauge factor

The resistivity, governed by the hopping transport mechanism, can be expressed as below;

$$\rho = \rho_0 e^{\beta l} \quad (1)$$

When characterized in resistance terms, eq (1) can be converted into eq (2):

$$\Delta R = R_f - R_i = \frac{L}{A} \rho_0 (e^{\beta(l + \Delta l)}) - \frac{L}{A} \rho_0 (e^{\beta l}) = \frac{L}{A} \rho_0 e^{\beta l} (e^{\beta \Delta l} - 1) \quad (2)$$

Generally, the strain and gauge factor are defined as below;

$$\varepsilon = \frac{\Delta l}{(l + d)} \quad (3)$$

$$G \equiv \beta(l + d) \quad (4)$$

When substituting eq (3) and (4) into eq (2), we can derive the concluding equation:

$$\frac{\Delta R}{R_i} = e^{\beta(l + d)\varepsilon} - 1 = e^{G\varepsilon} - 1 \approx G\varepsilon \quad (5)$$

ρ : conductivity, ρ_0 : pre-exponential constant, β : tunneling decay constant, l : interparticle distance, Δl : change of interparticle distance, R_f : resistance after strain, R_i : resistance before strain, ΔR : resistance changes, L : channel length of sensor, A : cross sectional area of sensor, ε : strain, d : particle diameter, G : gauge factor

The effect of various ligands for AgNC thin film based strain sensor

We also examined several types of ligands, including EDT, 1,3-Propanedithiol (PDT), 1,4-Butanedithiol (BDT), Benzene-1,2-dithiol, thioglycolic acid, and MPA (Figure S3a). As the length of ligand was increased, the gauge factor was also increased. Acid type ligands showed higher gauge factors than thiol based ligands, and MPA treatment shows the highest gauge factor.

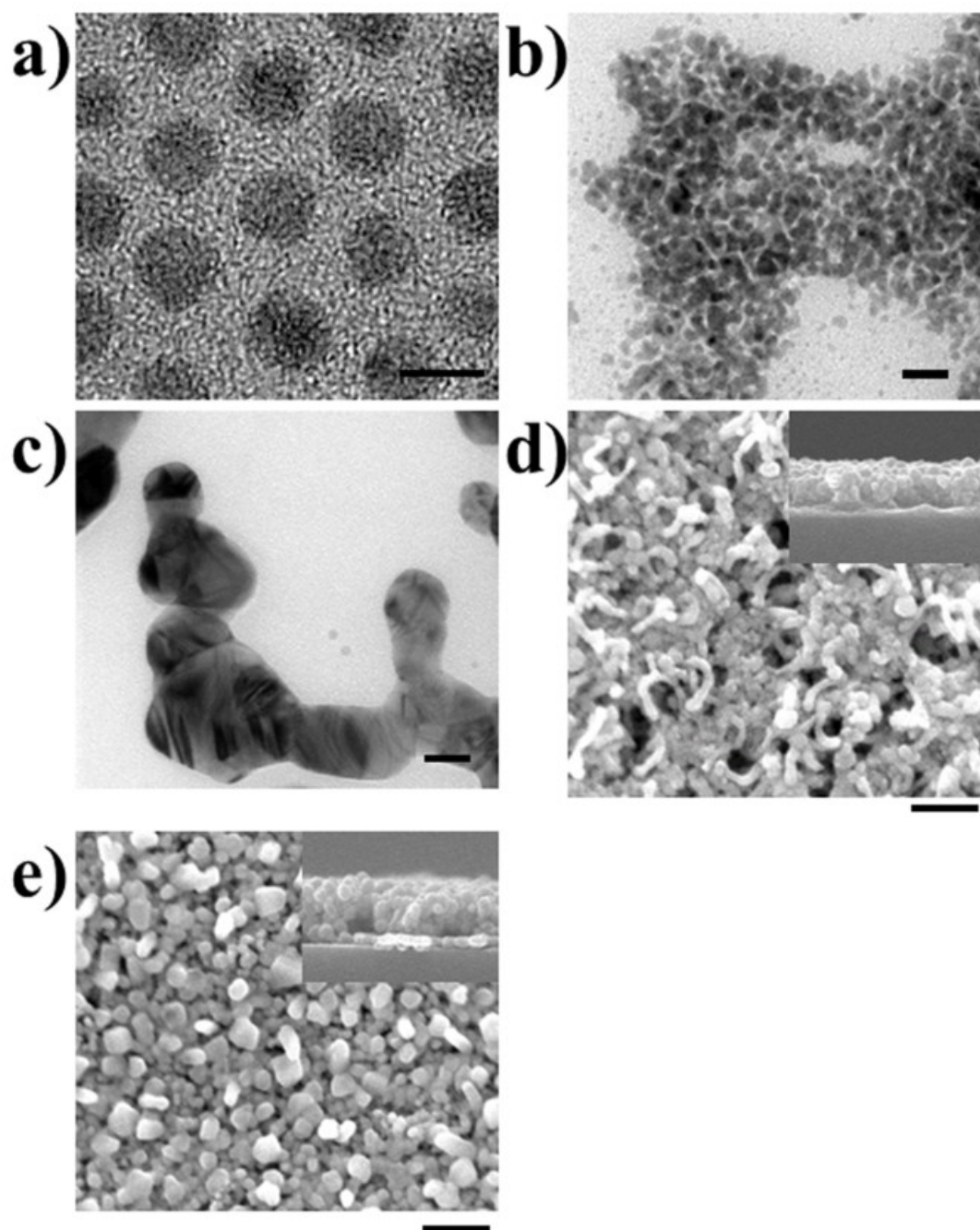


Fig. S1 TEM images of (a) as synthesized, (b) MPA-treated and (c) Cl-treated (right) Ag NCs (Scale bar in (a) 5nm, in (b, c) : 20 nm). SEM images of (d) Br-treated, and (e) Cl-treated Ag NC thin films (Scale bar : 500 nm).

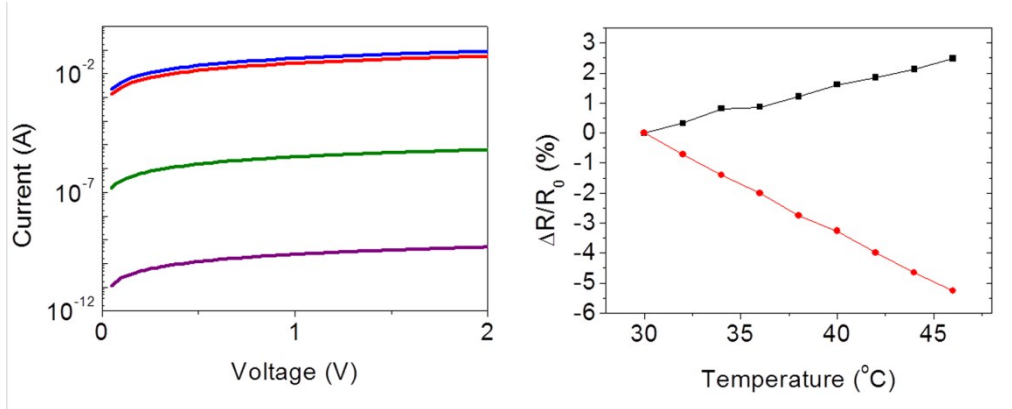


Fig. S2 (a) I-V curves of Br-treated (blue), Cl-treated (red), EDT-treated (green), and MPA-treated (purple) Ag NC thin films. (b) Resistance change of Br-treated (black) and MPA-treated (red) Ag NC thin films as a function of temperature. [Ref : 51]

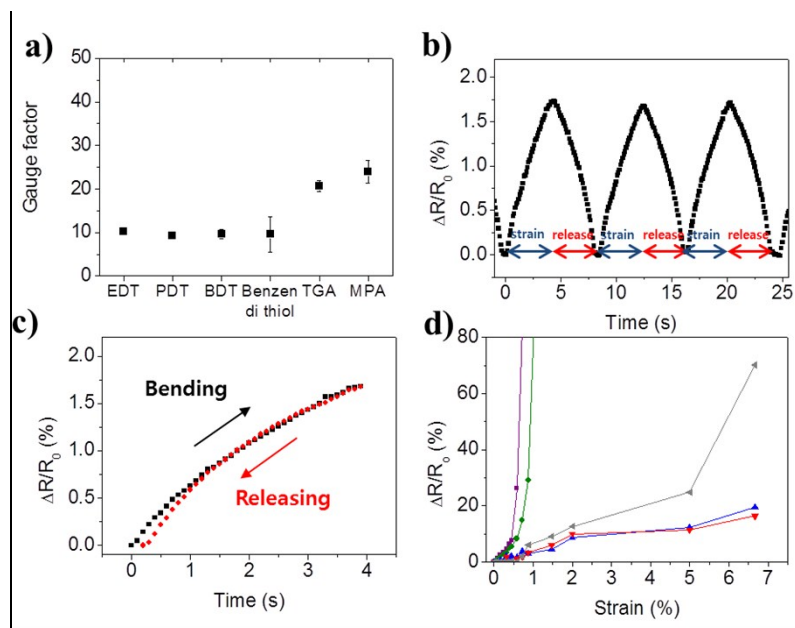


Fig. S3 (a) Gauge factors of various organic ligands treated Ag NC thin films. (b) Resistance response of MPA treated Ag NC thin films when 0.1% strain is applied and released slowly. (c) Hysteresis plot of MPA treated Ag NC thin films with 0.1% strain (black) applied and (red) released. (d) Resistance change of Ag NC thin films treated with MPA (purple), EDT (green), Cl (red), Br (blue) and E-beam evaporated (grey) as positive strain applied.

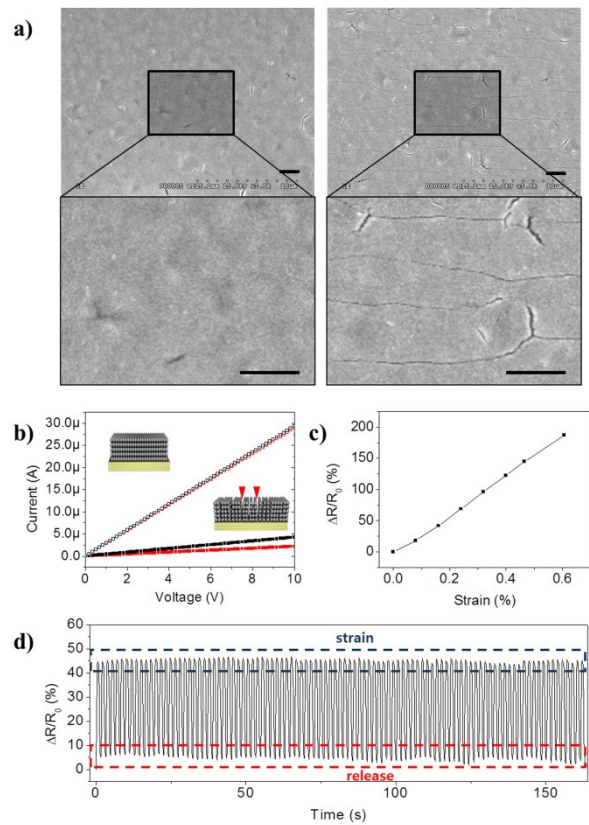


Fig. S4 (a) Large sized SEM image of Ag NCs thin films before (left) and after (right) crack formation by pre-strain (scale bar: 2 μm) (b) I-V curves of Ag NC thin films without (black) or with (red) applied strain and fabricated without (open symbol) or with (closed symbol) 2% applied pre-strain 10 times. (c) Resistance change of MPA treated and 2% applied pre-strain Ag NC thin films as a function of applied strain. (d) Response profile for MPA treated and pre-strained Ag NC thin films with 0.2% strain applied and released 100 times.

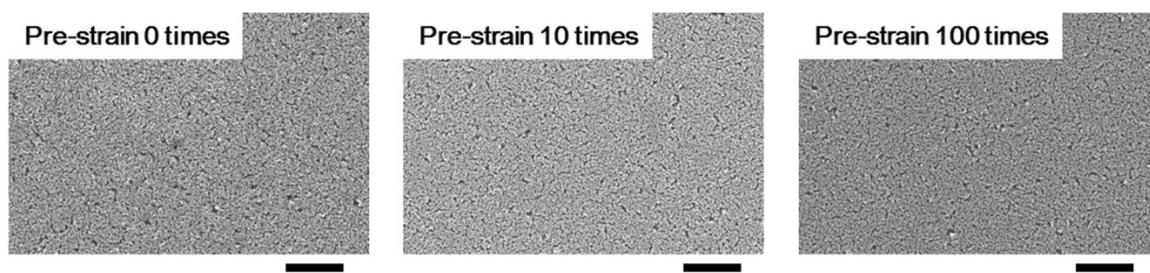


Fig. S5 SEM images of Br treated Ag NC thin films by applying 2% pre-strain 0 time (left), 10 times (middle), or 100 times (right) (Scale bar: 10 μm).



Fig. S6 Image of strain sensor mounted on wrist

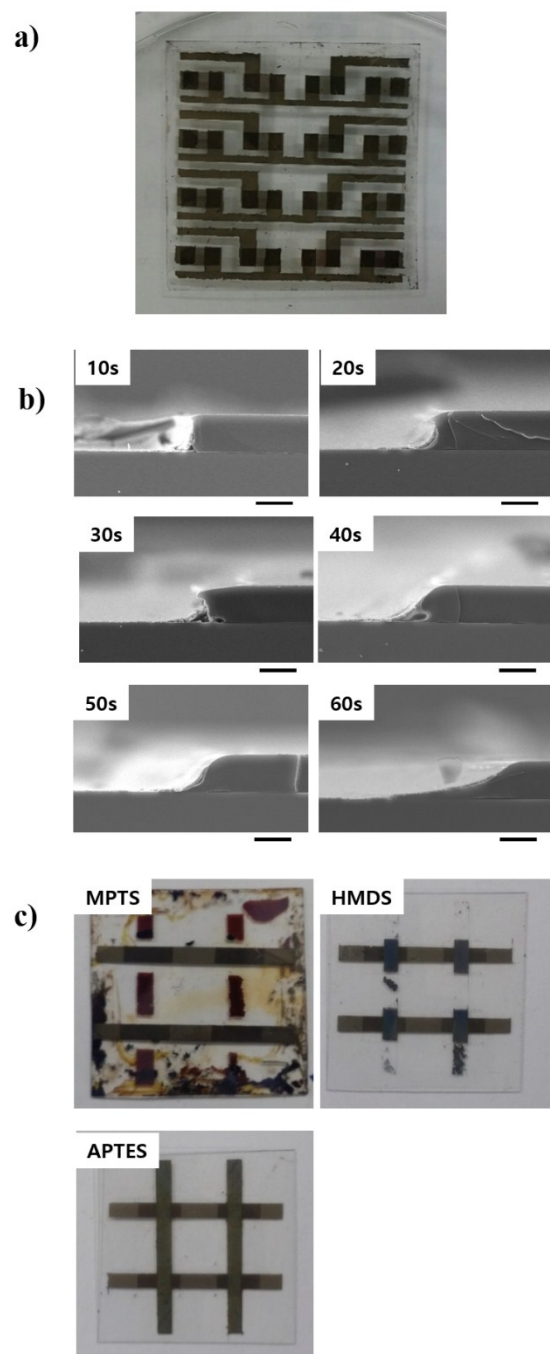


Fig. S7 (a) Photo image of 2D structured multi array sensor. (b) SEM cross section images of SU8 pattern as a function of exposure time (Scale bar : 10 μm). (c) MPTS-treated (left), HMDS-treated (middle), and APTES-treated (right) SU8 & PET with top and bottom Ag NC thin film electrodes.

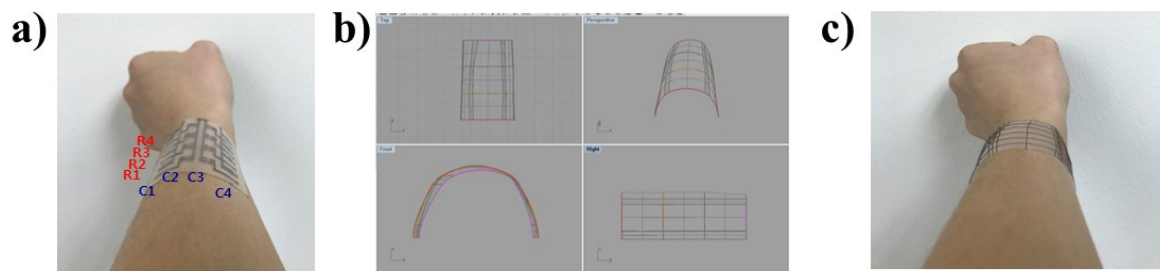


Fig. S8 (a) Image of multi array strain sensors on the wrist, (b) Design and drawing the shape of wrist based on the curvature at each points measured from the strain sensors, (c) reconstruction of the shape of the part of wrist.

Table S1 Curvature at each point in multi array strain sensor device on arm.

Curvature (1/radius)	C1	C2	C3	C4
R1	0.082	0.131	0.138	0.067
R2	0.095	0.146	0.148	0.062
R3	0.071	0.134	0.137	0.055
R4	0.104	0.156	0.213	0.074